

CoD: A Diffusion Foundation Model for Image Compression

Zhaoyang Jia^{1*} Zihan Zheng^{1*} Naifu Xue² Jiahao Li³ Bin Li³
 Zongyu Guo³ Xiaoyi Zhang³ Houqiang Li¹ Yan Lu³

¹ University of Science and Technology of China ² Communication University of China
³ Microsoft Research Asia

{jzy_ustc, zzh2003}@mail.ustc.edu.cn, lihq@ustc.edu.cn, {aaronxuenf}@cuc.edu.cn
 {libin, li.jiahao, zongyuguo, xiaoyizhang, yanlu}@microsoft.com

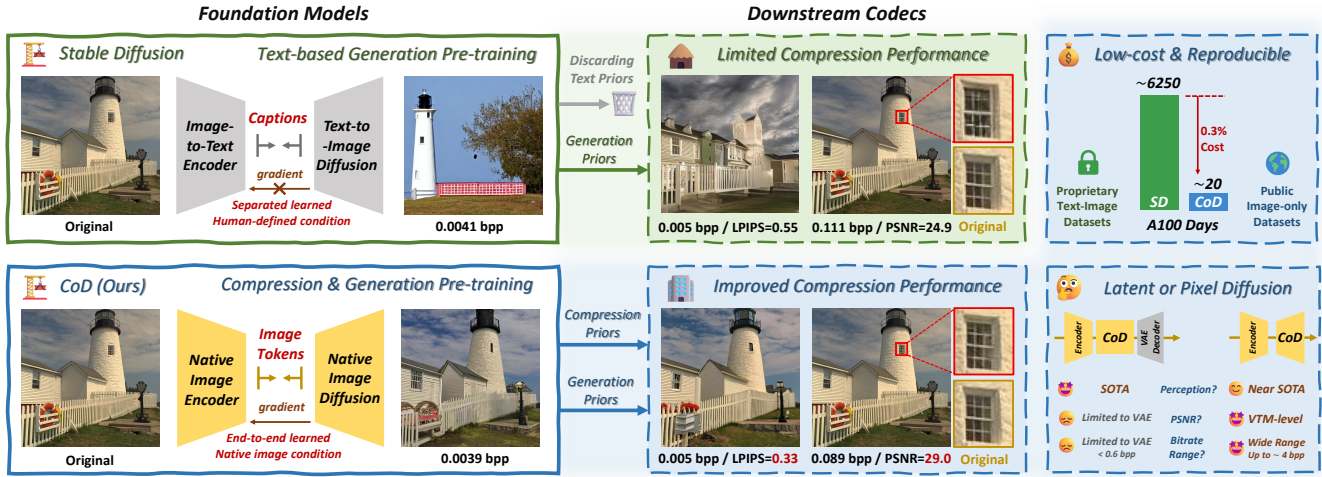


Figure 1. Overview of **Compression-oriented Diffusion** (CoD) foundation models, which are trained from scratch to jointly optimize compression and generation. Rather than a fixed codec, CoD serves as a foundational model for downstream diffusion-based codecs such as DiffC [42], substantially enhancing their performance by replacing Stable Diffusion.

Abstract

Existing diffusion codecs typically build on text-to-image diffusion foundation models like Stable Diffusion. However, text conditioning is suboptimal from a compression perspective, hindering the potential of downstream diffusion codecs, particularly at ultra-low bitrates. To address it, we introduce **CoD**, the first **Compression-oriented Diffusion** foundation model, trained from scratch to enable end-to-end optimization of both compression and generation. CoD is not a fixed codec but a general foundation model designed for various diffusion-based codecs. It offers several advantages: **High compression efficiency**, replacing Stable Diffusion with CoD in downstream codecs like DiffC achieves SOTA results, especially at ultra-low bitrates (e.g., 0.0039 bpp); **Low-cost and reproducible training**, 300× faster training than Stable Diffusion (~ 20 vs. $\sim 6,250$ A100 GPU days) on entirely open

image-only datasets; **Providing new insights**, e.g., We find pixel-space diffusion can achieve VTM-level PSNR with high perceptual quality and can outperform GAN-based codecs using fewer parameters. We hope CoD lays the foundation for future diffusion codec research. Codes will be released.

1. Introduction

Diffusion image compression [7, 15, 26, 31, 36, 45, 52] exploits the strong generative priors of denoising diffusion models [21, 32, 41] to achieve realistic image reconstruction. To inherit such generative priors, recent diffusion codecs typically adopt large-scale pretrained text-to-image diffusion models such as Stable Diffusion [38], demonstrating impressive performance in generative image compression.

However, when using text-to-image diffusion models in compression, the role of text conditions remains unclear. Although early works such as Text+Sketch [28] and PerCo [7]

*This work was done when Zhaoyang Jia and Zihan Zheng were full-time interns at Microsoft Research Asia.

claim image captions can serve as a high-level semantic signal to facilitate ultra-low bitrate compression, later studies [15, 51] demonstrate that fine-tuning Stable Diffusion to discard text priors can further improve compression efficiency. Additional evidence comes from the zero-shot diffusion compression framework DiffC [45], which theoretically measures the “compression capability” of a denoising diffusion model. When applied to Stable Diffusion, DiffC reveals that text conditions are detrimental to compression performance, especially at low bitrates. These observations suggest that text-conditioned diffusion models are not naturally suitable for compression, and that **Stable Diffusion is not the ideal foundation model for diffusion codecs**.

To understand this phenomenon, we analyze the underlying mechanism. In a standard compression formulation,

$$y = \text{Encode}(x, \Theta), \quad \hat{x} = \text{Decode}(y, \Phi) \quad (1)$$

where x , y , and \hat{x} denote the original image, compressed representation, and reconstruction, respectively, and Θ and Φ represent the trained parameters of the encoder and decoder. If we set Θ as an image captioner like BLIP-2 [29] and Φ as Stable Diffusion, we note that *text-conditioned diffusion can be formulated in the compression formulation*, as illustrated in the top left of Figure 1. From the perspective of compression, text conditions introduce two limitations. First, human-generated text is less efficient in describing fine-grained spatial and texture details of natural images. Second, the discrete vocabularies in text is non-differentiable to prevent joint optimization of Θ and Φ , thus making rate-distortion optimization inapplicable.

Recognizing the limitations of text conditions, a natural next step is to **train a diffusion foundation model explicitly oriented toward compression**. Neural codecs can learn compact, native image tokens as conditions for diffusion models, and enable end-to-end training with the diffusion model to determine the optimal image representations for coding. By carefully designing and leveraging advanced diffusion training algorithms, we introduce the first **Compression-oriented Diffusion** foundation model, **CoD**. The architecture of CoD is simple yet effective: a native image encoder Θ to compress images into tokens, followed by an information bottleneck, and a diffusion model Φ to decode pixels conditioned on these image tokens. The bottleneck is designed to enforce ultra-low bitrates (e.g., 0.0039 bpp), transmitting only essential semantic information while allowing the diffusion model the flexibility to generate realistic details. As illustrated in the bottom left of Figure 1, CoD achieves significantly higher reconstruction fidelity compared to text-to-image foundation models.

It is worth noting that CoD is not a fixed codec but a general foundation model designed for diverse diffusion-based compression algorithms. In practice, it can replace Stable Diffusion in existing downstream diffusion codecs

to improve performance. Unlike Stable Diffusion that only provides generation priors, CoD additionally learns compression priors to substantially boost downstream performance, particularly at low bitrates. CoD offers several advantages:

Low Training Cost. Compared to Stable Diffusion, CoD is far more efficient to train. Stable Diffusion v1.5 requires about 6,250 A100 GPU days [8], whereas CoD only takes around 20 A100 GPU days (0.3% cost). Unlike text-to-image diffusion that relies on text-image training pairs, CoD is fully self-supervised and only requires image datasets, making it easier to scale. Furthermore, while Stable Diffusion uses proprietary datasets, CoD is trained entirely on open datasets such as ImageNet [39], OpenImages [25], and SA-1B [24], making it easy to reproduce and unleashing the potential for future exploration across different diffusion codec architectures and training schemes.

Providing New Insights. We conduct an in-depth analysis of CoD to gain insights into diffusion-based compression. We facilitate scaling-law study of CoD to reveal how model size affects compression performance. We further show that diffusion codecs can surpass GAN-based codecs even with significantly fewer parameters. In addition, we present a comprehensive comparison between pixel-space and latent-space diffusion. While latent diffusion offers superior perceptual quality at low bitrates, its PSNR and bitrate range are constrained by the VAE (e.g., up to \sim 26 dB PSNR at 0.6 bpp). In contrast, pixel diffusion delivers both high perceptual quality and high PSNR across a wide bitrate range (e.g., reaching near-lossless \sim 47 dB PSNR at 4 bpp).

High Compression Performance. As a compression-oriented foundation model, CoD enables high-performance downstream codecs. In this paper, we evaluate it using the state-of-the-art zero-shot diffusion compression method, DiffC [42, 45]. Compared to Stable Diffusion, DiffC with CoD achieves significantly better performance, especially at low bitrates. With pixel-space CoD, it even matches VTM [46] in PSNR while outperforming previous pixel-space perceptual codecs such as MS-ILLM [35] in FID. The qualitative results in middle column of Figure 1 demonstrate that pixel-space CoD achieves much higher reconstruction fidelity, highlighting the potential of pixel diffusion to approach the theoretical rate-distortion-perception trade-off.

The contributions of this work can be summarized as:

- We introduce the first compression-oriented diffusion foundation model, CoD, designed to replace Stable Diffusion in diffusion codecs.
- CoD enables low-cost, reproducible training, supporting exploration of new network architectures.
- CoD delivers high compression performance, especially on ultra-low bitrates.
- CoD pushes the boundaries of diffusion codecs, demonstrating the potential of pixel-space diffusion as a pathway toward the optimal rate-distortion-perception trade-off.

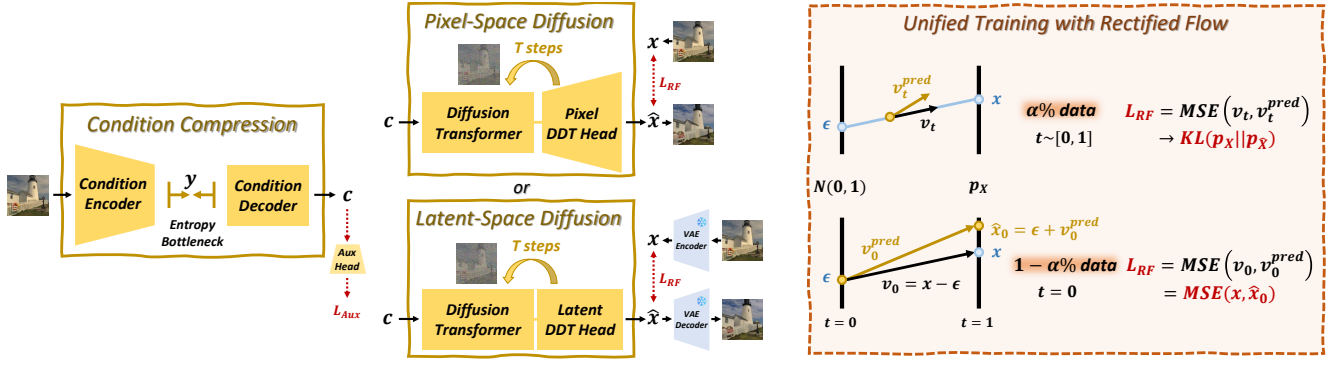


Figure 2. Framework overview of CoD in pixel and latent spaces. CoD consists of a condition encoder, an entropy bottleneck, a condition decoder and a diffusion model which is decoupled to DiT backbone and DDT head [48]. CoD is trained with rectified flow [32], where $1 - \alpha\%$ samples are trained at $t = 0$ to jointly optimize distortion and perception.

2. Compression-oriented Diffusion

In this section, we introduce the implementation details of the proposed compression-oriented diffusion models, CoD.

2.1. Pipeline

We implement CoD in both pixel and latent spaces. As illustrated in Figure 2, given an input data x , CoD performs: **Condition Encoding**. An encoder firstly compresses x into compact representations. Following [12], we stack residual blocks [18] and attention layers [44] to construct the encoder. The output is at $1/32$ resolution of the original images.

Entropy bottleneck. It is designed to maintain an ultra-low bitrate for y , encouraging the diffusion model to learn strong generative capabilities. This can be implemented as scalar quantization with entropy models [5], vector quantization [12], or finite scalar quantization [34]. For simplicity, we use vector quantization with a codebook size of $N = 2^4 = 16$, corresponding to $4\text{bpp}/(32 \times 32) = 0.0039 \text{ bpp}$.

Condition Decoding. The condition decoder reconstructs intermediate compression conditions c from the image tokens y . The decoder adopts similar structures as the encoder. The condition c is at a $1/16$ resolution of the original image.

Diffusion-based reconstruction. The diffusion module denoises a randomly sampled Gaussian noise over T steps under the guidance of condition c to reconstruct \hat{x} . Following DDT [48], we decouple DiT backbone and DDT head to enhance capacity. DDT performs denoising at $1/16$ resolution, where the condition c is concatenated with the noised input along the channel dimension at each step for guidance.

In the latent space, since VAE latents are already at $1/8$ resolution, we apply a 2×2 patch embedding to downsample them to $1/16$, and upsample the output of DDT head back to $1/8$ before passing to the VAE decoder. In the pixel space, we directly use a 16×16 patch embedding to map the noised images to $1/16$ resolution, and adopt the pixel DDT head from [47], where each feature predicts a neural field that

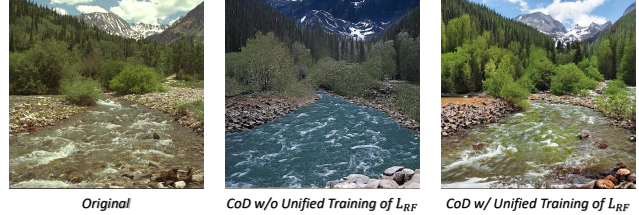


Figure 3. Effects of unified training with rectified flow.

reconstructs a corresponding 16×16 patch. Since the DiT backbone runs at $1/16$ resolution of original images, **pixel-space CoD has a similar computation complexity as in latent space**. Details are in the supplementary material.

2.2. Diffusion Training

Preliminary. Denoising diffusion models [45] model the data distribution by progressively perturbing a clean sample x with Gaussian noise ε , transforming $p(x)$ into a standard Gaussian distribution. At timestep t , it is formulated as,

$$x_t = \alpha_t x + \sigma_t \varepsilon, \quad \varepsilon \sim \mathcal{N}(0, I) \quad (2)$$

where α_t and σ_t define the noise schedule. The process can be expressed as a stochastic differential equation (SDE),

$$dx_t = f(t) x_t dt + g(t) d\omega_t \quad (3)$$

with drift $f(t)$ and diffusion $g(t)$ determined by α_t and σ_t . Score-based models [41] learn the score function of $p(x)$ to solve the reverse SDE and generate samples.

Rectified Flow (RF) [32] reinterprets diffusion as a deterministic transformation. It removes the stochastic term from the SDE and adopts a linear transition schedule:

$$x_t = t \cdot x + (1 - t) \cdot \varepsilon. \quad (4)$$

So the trajectory follows a simple ordinary differential equation (ODE) formulated as:

$$dx_t = v_t dt, \quad \text{where } v_t = x - \varepsilon \quad (5)$$

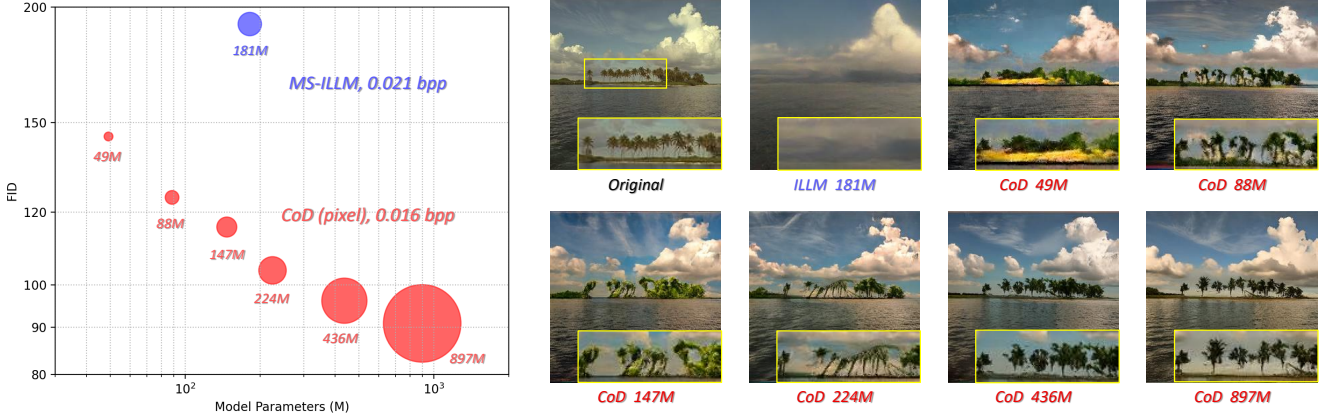


Figure 4. Scaling law analysis on the Kodak dataset at a resolution of 256×256 . All CoD models are at 0.016 bpp while MS-ILLM is at 0.021 bpp. FID is computed over overlapping 64×64 patches following [36].

Instead of estimating the score, RF directly learns the velocity field v_t , providing more stable training, faster inference, and a clearer geometric view of generation.

Unified Training with Rectified Flow. CoD predicts the velocity v_t so it can be trained with the rectified flow loss,

$$\mathcal{L}_{\text{RF}} = \text{MSE}(v_t, v_t^{\text{pred}}) \quad (6)$$

where v_t^{pred} denotes the predicted velocity field. Theoretically, optimizing \mathcal{L}_{RF} reduces the Kullback–Leibler (KL) divergence between the reconstructed and original distributions [13], which can reflect the perception term in rate-distortion-perception (R–D–P) theory [6]. Hence, optimizing \mathcal{L}_{RF} naturally promotes perceptual quality.

However, we find that rectified flow loss mainly guarantee the reconstruction consistency of the structure instead of color information (see Figure 3). From a compression viewpoint, this is consistent with R–D–P theory: standard diffusion training neglects the distortion term, leading to limited reconstruction fidelity.

To overcome this, we introduce a unified formulation that integrates a distortion term into the rectified flow loss. Since the one-step estimate at $t = 0$ is $\hat{x}_0 = \varepsilon + v_0^{\text{pred}}$, the rectified flow loss can be rewritten given $v_0 = x - \varepsilon$:

$$\mathcal{L}_{\text{RF}} = \text{MSE}(v_0, v_0^{\text{pred}}) = \text{MSE}(x, \hat{x}_0) \quad (7)$$

Thus, optimizing \mathcal{L}_{RF} at $t = 0$ directly minimizes one-step reconstruction distortion to incorporate a distortion term during training. As illustrated in Figure 2, during training we randomly select $\alpha\%$ samples with $t \in [0, 1]$ and the rest with $t = 0$ to enable the unified training.

Discussion. Unified training is designed for continuous flows, where the probability of sampling a fully noised state $t = 0$ approaches zero. We observe that color reconstruction in CoD is largely determined by its first denoising step; thus, the absence of $t = 0$ optimization often leads to noticeable color shifts. In contrast, DDPM-based codecs such as

PerCo [7] employ discrete timesteps uniformly sampled as $t_{\text{DDPM}} \in 1, \dots, 1000$, inherently including optimizing of fully noised state. This can be viewed as a special case of our formulation with $1 - \alpha\% = 1/1000$.

2.3. Implementation Details

Datasets. Foundation models require large-scale training to achieve optimal performance. Unlike text-to-image generation that depends on text-image data pairs, CoD is fully self-supervised and requires only image datasets, making large-scale scaling more accessible. In this paper, we use ImageNet-21K [39], OpenImage [25] and SA-1B [24], including a total of 22M images. All datasets are publicly available, facilitating reproducibility for future research.

Loss Function. For the information bottleneck, we adopt the codebook commitment loss \mathcal{L}_{C} [12]. Diffusion training employs the rectified flow loss \mathcal{L}_{RF} and the representation alignment loss $\mathcal{L}_{\text{REPA}}$ with DINOv2 [37]. Additionally, an auxiliary head (Figure 2) reconstructs both original pixels and DINOv2 features from the condition c to enhance condition learning. Further analysis of this auxiliary loss \mathcal{L}_{aux} is in the supplementary material. The overall objective is

$$\mathcal{L} = \mathcal{L}_{\text{RF}} + \lambda \cdot \mathcal{L}_{\text{REPA}} + \beta \cdot \mathcal{L}_{\text{C}} + \gamma \cdot \mathcal{L}_{\text{aux}} \quad (8)$$

where $\lambda = 0.5$, $\beta = 0.25$ and $\gamma = 1.0$.

Training Details. We incorporate several advanced techniques for diffusion training. Timesteps are sampled following a log-normal distribution, which is further enhanced by the unified training strategy introduced in Section 2.2. CoD is progressively trained from low to high resolution: first at 256×256 for 400k steps with a batch size of 128, and then fine-tuned at 512×512 for 150k steps with a batch size of 64. The encoder downsamples images to $1/16$ at 256×256 resolution (0.0156 bpp) and to $1/32$ at 512×512 (0.0039 bpp), ensuring that the total number of patches and overall bit cost remain consistent.

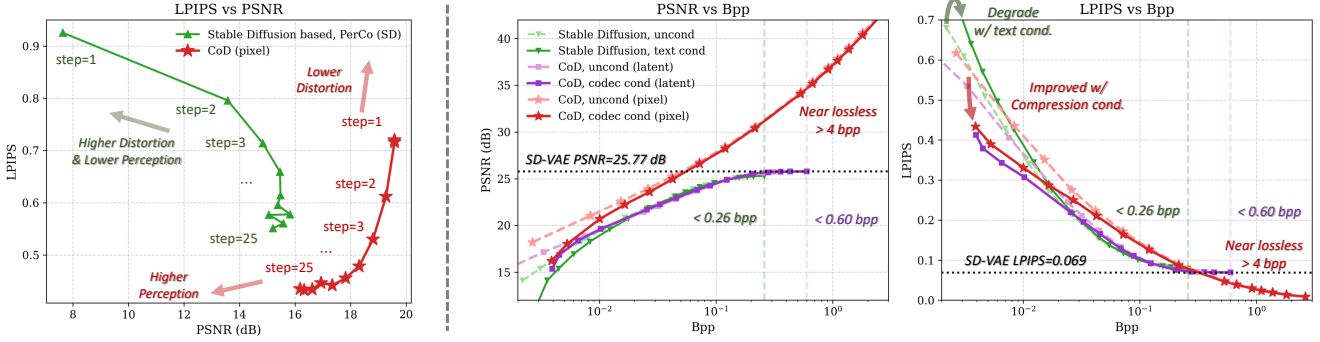


Figure 5. Comparison of CoD and Stable Diffusion on Kodak at 512×512 resolution. (left) Pixel-space CoD enables zero-shot distortion-perception controlling by adjusting the sampling steps. CoD is at 0.0039 bpp and PerCo is at 0.0036 bpp. (right) Text conditions harms performance of zero-shot algorithm DiffC on Stable Diffusion, while CoD condition boosts LPIPS at low-bitrate. In addition, pixel-space CoD is not limited by the SD-VAE thus demonstrating wider bitrates, higher PSNR and higher potential in perceptual quality.



Figure 6. Visual comparison between Stable-Diffusion-based codecs and latent-space CoD under ultra-low bitrates.

Training Costs. CoD is trained on 4 NVIDIA A100 GPUs for approximately 5 days, totaling around 20 A100 GPU days. This represents only about 0.3% of the training cost of Stable Diffusion v1.5 [38], primarily because: (1) CoD learns the most informative compression conditions end-to-end, rather than relying on high-dimensional, human-defined text embeddings; (2) the unified rectified flow training stabilizes and accelerates convergence; (3) advanced optimization strategies such as REPA [54] further improve efficiency.

Diffusion Sampling. For ODE-based sampling, we employ the Adam-like-2nd solver [47] with 25 steps. We use classifier-free guidance [20] with scales of 3.0 for pixel space and 1.25 for latent space to enhance conditional generation.

3. Analysis on Foundation Model

In this section, we conduct an in-depth analysis of CoD to investigate its performance and underlying characteristics. More analysis are in the supplementary material.

3.1. Evaluation

CoD naturally operates as a codec at 0.0039 bpp. We evaluate its compression performance on the Kodak [10] dataset at 512×512 resolution. To ensure fair comparison among foundation models, we employ the same SD-VAE and compare our latent-space CoD with Stable-Diffusion-based codecs, including zero-shot DiffC [45], DDCM [36], and fine-tuned PerCo (SD) [26] and OSCAR [15]. As shown in Figure 6, CoD achieves superior reconstruction quality. A more detailed quantitative comparison is presented in Section 4.

3.2. Scaling Law

Most diffusion codecs are constrained by the parameter count of Stable Diffusion (approximately 860M), making it difficult to study parameter scaling. It also remains unclear whether the performance advantages of diffusion codecs over GAN-based codecs (e.g., MS-ILLM [35]) stem from architectural improvements or simply from model scaling. To explore this, we train pixel-space CoDs with varying channel dimensions at 256×256 resolution for 400k steps and evaluate them on Kodak. As shown in Figure 4, we observe a clear trend: increasing model parameters consistently enhances compression performance. Compared with the GAN-based MS-ILLM (181M parameters), CoD achieves notably better reconstruction quality even with only 49M parameters, confirming that the performance gain primarily originates from algorithmic improvements rather than model size.

3.3. Zero-Shot Distortion-Perception Control

The proposed unified training jointly optimizes one-step distortion and multi-step perception, endowing CoD with the ability to control the distortion-perception trade-off directly through the number of sampling steps. As shown in Figure 5 (left), at 0.0039 bpp, pixel-space CoD attains the best perceptual quality at 25 steps and achieves a 3.4 dB PSNR improvement (from 16.2 dB to 19.6 dB) when reduced to a

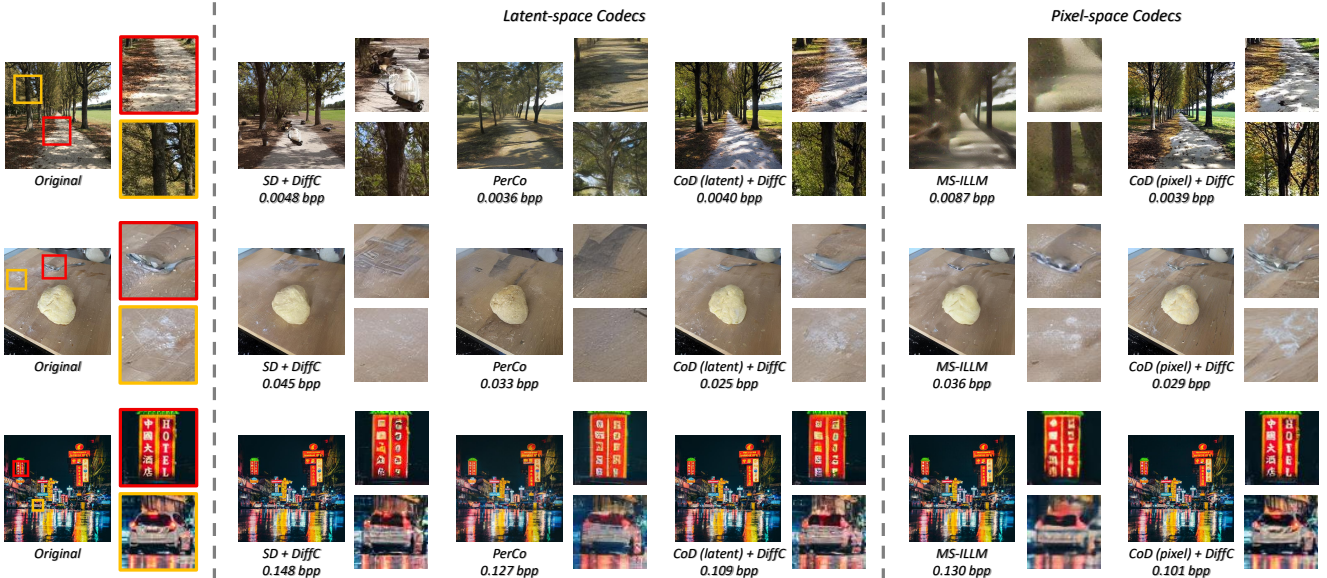


Figure 7. Visualization comparison on the CLIC2020 test set across bitrates from low (top) to high (bottom).

single step. Intermediate step counts smoothly interpolate between these two states. In contrast, diffusion codecs without this formulation (e.g., PerCo (SD)) fail to exhibit such controllable improvement through step reduction.

3.4. Revisiting Pixel-Space Diffusion

Recent diffusion codecs typically operate in the latent space of a KL-VAE, achieving impressive results at low bitrates (e.g., <0.1 bpp). However, their performance is fundamentally constrained by the entropy and reconstruction capacity of the underlying VAE. As shown in Figure 5 (right), DiffC [45] built on Stable Diffusion cannot surpass the reconstruction limit of the SD-VAE (PSNR 25.77 dB, LPIPS 0.069), with a bitrate ceiling around 0.26 bpp. Similarly, latent-space CoD remains bounded by VAE quality even up to 0.60 bpp, indicating that latent diffusion codecs inherently operate within a limited quality and bitrate range.

In contrast, pixel-space CoD directly models raw pixels to overcome this constraint. It can scale the bitrate beyond 1.0 bpp while continuously improving reconstruction quality. Pixel-space CoD surpasses latent diffusion models in LPIPS at around 0.3 bpp and maintains substantially higher PSNR across the entire range. This demonstrates the potential of pixel-space diffusion as a more general and unconstrained approach to learned compression in future research.

4. Downstream Compression Performance

In this section, we conduct a comprehensive evaluation of CoD when integrated into downstream compression frameworks. Since most diffusion-based codecs do not release their training code, we employ the zero-shot compression method DiffC [45] on CoD for comparison.

Benchmarks and Baselines. Experiments are conducted on the Kodak [10], CLIC2020 test set [43] and Div2K [1]. All images are resized and center-cropped to a resolution of 512×512 . We report distortion using PSNR and perceptual quality using LPIPS [55], DISTs [9], and FID [19]. Following [36], FID is computed on extracted patches (64×64 for Kodak and 128×128 for CLIC2020). Bitrate is measured in bits per pixel (bpp). In addition to diffusion codecs (DiffC, DDCM, PerCo (SD), and OSCAR; see Section 3.1), we further compare against the latent-space codec DiffEIC [31] and pixel-space codecs including the traditional codec VTM [46] and perceptual codecs HiFiC [33], MS-ILLM [35], CDC [52] and TACO [27]. We also discuss StableCodec [56] and OneDC [51] which are built on pretrained one-step diffusion models in the supplementary.

Pixel-space Comparison. The rate-distortion curves on pixel space codecs are shown in Figure 8. Pixel space codecs are free of the limitation of VAE latents thus can achieve wider bitrates and quality ranges. Across all bitrates, our codec achieves superior PSNR, DISTs and FID values. Notably, perceptual codecs HiFiC, MS-ILLM, CDC ($\rho = 0.9$) and TACO are optimized with LPIPS, whereas pixel-space CoD is not, which explains performance on LPIPS.

Surprisingly, our codec achieves comparable BPP-PSNR performance to VTM (BD-Rate is -2.1% using VTM as anchor) while delivering significantly better perceptual quality. In contrast, HiFiC, MS-ILLM and CDC ($\rho = 0.9$) improve perceptual quality at the expense of PSNR. TACO removes the GAN [14] loss to balance distortion and perception, but fails to achieve an optimal trade-off. By comparison, DiffC with pixel-space CoD attains the best balance across all bitrates. Although pixel diffusion has been less explored than latent diffusion, our results demonstrate that **CoD high-**

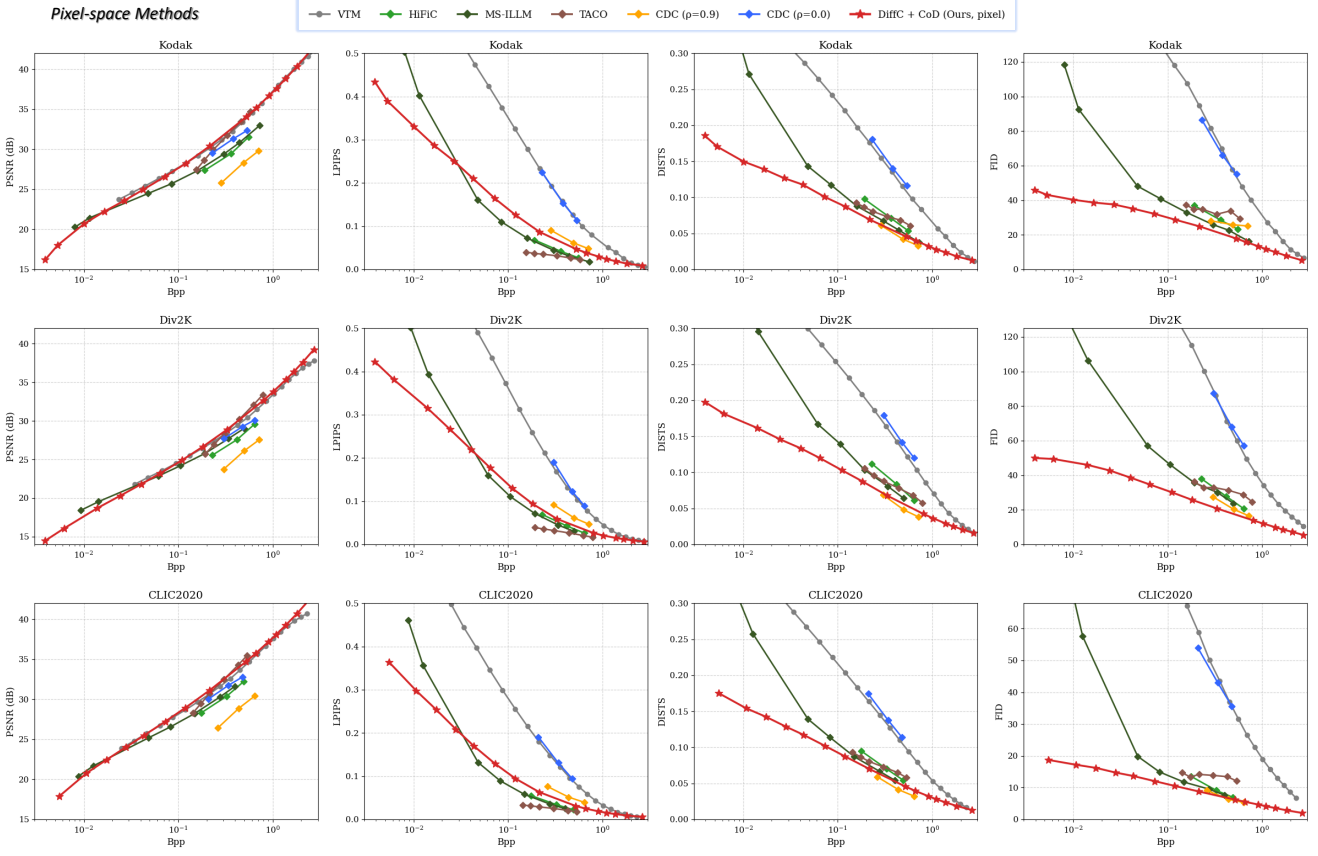


Figure 8. Comparison with pixel-space codecs. Note: HiFiC, MS-ILLM, CDC, and TACO are optimized using LPIPS, whereas CoD is not. So pixel-space CoD may not achieve the best LPIPS at certain bitrates, despite outperforming in PSNR, DISTS and FID.

lights the potential of pixel diffusion to achieve a superior rate-distortion-perception trade-off.

Latent-space Comparison. The rate-distortion curves on latent space codecs are shown in Figure 9. Compared to existing latent-space codecs, DiffC with latent-space CoD achieves the best reconstruction quality at lower bitrates (e.g., <0.02 bpp). At higher bitrates, the gap narrows as performance approaches the SD-VAE limit. At some points (e.g., FID at 0.02 bpp on CLIC), CoD performs slightly worse than DiffC due to smaller training scale, which can likely be closed with larger data and training in the future.

Visualization. Figure 7 compares visual results across different bitrates among SD-based DiffC, PerCo (SD), and the pixel-space MS-ILLM. At low bitrates, CoD achieves higher fidelity than SD-based codecs and more realistic details than prior pixel-space methods. At high bitrates, latent codecs are constrained by the reconstruction quality of SD-VAE, e.g., small characters appear heavily distorted, while MS-ILLM also struggles to recover clear text. In contrast, pixel-space CoD reconstructs sharp and accurate details, demonstrating the strong potential of pixel-space diffusion.

5. Related Works

5.1. Generative Image Compression

Unlike neural image codecs [4, 5, 16] that primarily minimize reconstruction distortion (MSE), generative image compression [2, 3, 17, 22, 23, 50] aims to achieve both low distortion and high perceptual quality. Early works [33, 35] introduced conditional GANs to enhance perceptual realism, successfully improving perceptual quality compared to MSE-optimized codecs, albeit at the cost of higher reconstruction distortion. TACO [27] further incorporates textual information to mitigate MSE degradation, yet still falls short in achieving an ideal distortion–perception balance. To the best of our knowledge, we are the first to demonstrate that pixel-space diffusion can attain VTM-level distortion while delivering superior perceptual quality to GAN-based codecs.

5.2. Diffusion Image Compression

Recent advances in generative image compression increasingly leverage the powerful generative priors of diffusion models to achieve higher realism. PerCo [7] compresses image representations and text captions as conditions, fine-tuning a pretrained latent diffusion model for perfect realism.

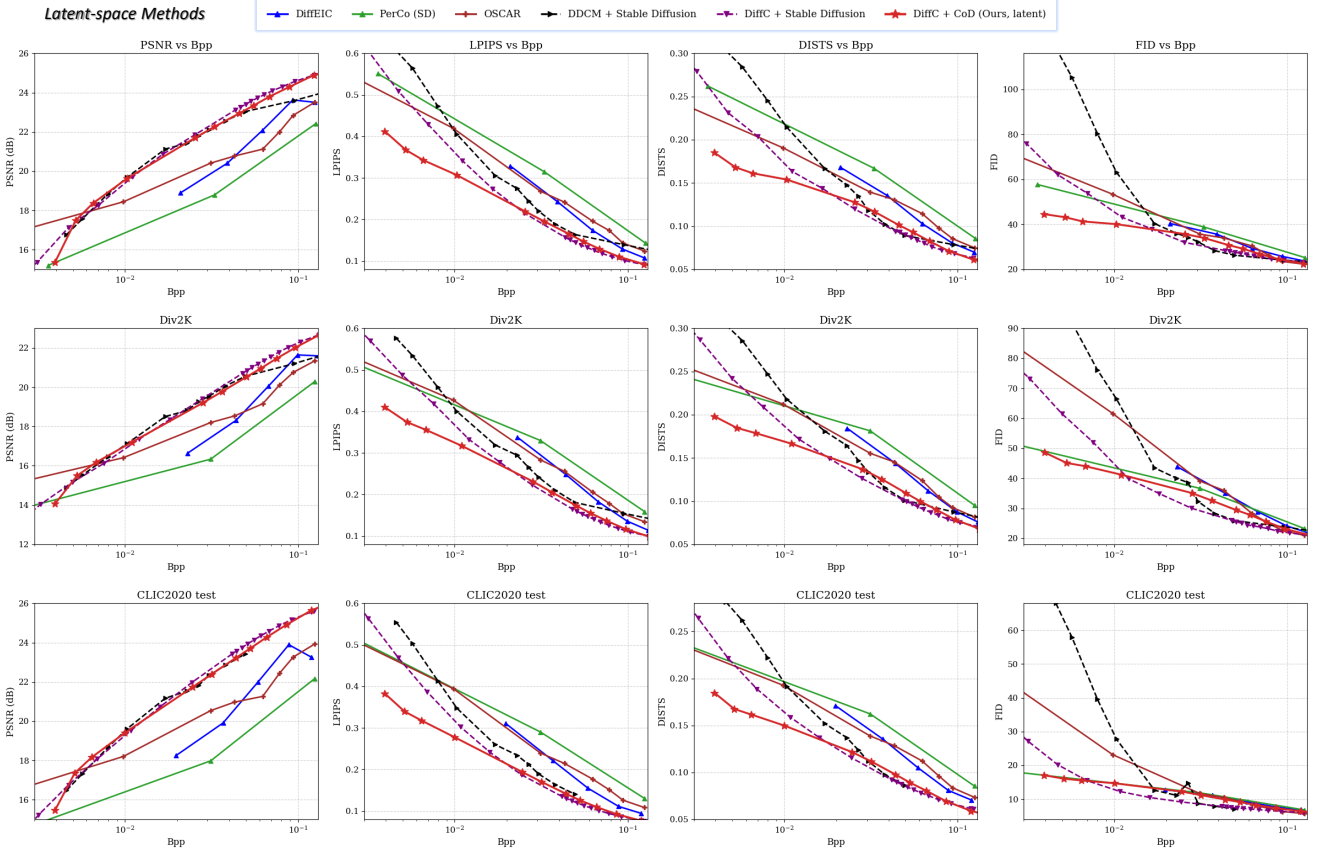


Figure 9. Comparison with latent-space codecs. Latent-space CoD demonstrates state-of-the-art performance towards low bitrates.

In contrast, DiffEIC [31] and OSCAR [15] show that removing the text bitstream can yield better overall performance. Other approaches [11, 49] investigate zero-shot compression using pretrained diffusion models without fine-tuning. DiffC [42, 45] introduces reverse-channel coding to progressively compress increasingly noised representations, while DDCM [36] adopts random codebooks to encode the random sampled noises. Most of these methods depend on pretrained diffusion foundation models such as Stable Diffusion, which are theoretically suboptimal for compression. CoD offers an alternative, compression-oriented diffusion foundation model that can serve as a stronger backbone for such approaches, enabling superior performance.

Another early exploration on pixel-space diffusion codec is CDC [52], which also formulates compression as conditions for diffusion. However, CoD differs in several key aspects. First, CoD emphasizes training at ultra-low bitrates (~ 0.0039 bpp) to strengthen its strong generative prior, and it relies purely on diffusion loss rather than traditional perceptual losses. In contrast, CDC is trained at high bitrates (> 0.2 bpp), where dense information limits generative learning. Consequently, CDC requires perceptual losses such as LPIPS, otherwise its perceptual quality drops to the level of an MSE-optimized codec. Second, CoD embodies the

concept of a foundation model, scaling training to push the frontier of compression research, while CDC does not consider scaling laws. Finally, CoD offers insights beyond the model itself: we provide a comprehensive analysis of scaling behavior, pixel- vs. latent-space and conditioning modalities, offering broader insights for future research.

6. Conclusion and Limitation

To conclude, we present CoD, the first compression-oriented diffusion foundation model. CoD is trained from scratch and enables end-to-end joint optimization of compression and diffusion generation, substantially improving diffusion-based compression performance, particularly at ultra-low bitrates. CoD is trained entirely on open datasets with low computational cost, facilitating reproducibility and further research. Building on CoD, we investigate the scaling laws of diffusion codecs and demonstrate the potential of pixel-space diffusion towards strong R–D–P trade-off across a wide bitrate range. We believe CoD establishes a solid foundation for future advances in diffusion-based compression.

Despite these advantages, CoD still has several limitations at this stage. First, it is not yet trained for high-resolution inputs. Although extending CoD to higher resolutions (e.g., 2K) is technically feasible, it would require substantially

higher computational cost. As an early academic prototype, we leave this for future work. Second, similar to all diffusion codecs, CoD does not meet real-time coding requirements. Nevertheless, as shown in Section 3.2, even a compact CoD model already surpasses GAN-based codecs by a large margin. With continued advances in diffusion distillation, we hope real-time will become attainable in the near future.

References

[1] Eirikur Agustsson and Radu Timofte. Ntire 2017 challenge on single image super-resolution: Dataset and study. In *Proceedings of the IEEE conference on computer vision and pattern recognition workshops*, pages 126–135, 2017.

[2] Eirikur Agustsson, Michael Tschannen, Fabian Mentzer, Radu Timofte, and Luc Van Gool. Generative adversarial networks for extreme learned image compression. In *Proceedings of the IEEE/CVF International Conference on Computer Vision*, pages 221–231, 2019.

[3] Eirikur Agustsson, David Minnen, George Toderici, and Fabian Mentzer. Multi-realism image compression with a conditional generator. In *Proceedings of the IEEE/CVF Conference on Computer Vision and Pattern Recognition*, pages 22324–22333, 2023.

[4] Johannes Ballé, Valero Laparra, and Eero P Simoncelli. End-to-end optimized image compression. In *5th International Conference on Learning Representations, ICLR 2017*, 2017.

[5] Johannes Ballé, David Minnen, Saurabh Singh, Sung Jin Hwang, and Nick Johnston. Variational image compression with a scale hyperprior. In *International Conference on Learning Representations*, 2018.

[6] Yochai Blau and Tomer Michaeli. Rethinking lossy compression: The rate-distortion-perception tradeoff. In *International Conference on Machine Learning*, pages 675–685. PMLR, 2019.

[7] Marlene Careil, Matthew J. Muckley, Jakob Verbeek, and Stéphane Lathuilière. Towards image compression with perfect realism at ultra-low bitrates. In *The Twelfth International Conference on Learning Representations*, 2024.

[8] Junsong Chen, Jincheng YU, Chongjian GE, Lewei Yao, Enze Xie, Zhongdao Wang, James Kwok, Ping Luo, Huchuan Lu, and Zhenguo Li. Pixart-\$\alpha\$: Fast training of diffusion transformer for photorealistic text-to-image synthesis. In *The Twelfth International Conference on Learning Representations*, 2024.

[9] Keyan Ding, Kede Ma, Shiqi Wang, and Eero P Simoncelli. Image quality assessment: Unifying structure and texture similarity. *IEEE transactions on pattern analysis and machine intelligence*, 44(5):2567–2581, 2020.

[10] Eastman Kodak Company. Kodak lossless true color image suite. <http://r0k.us/graphics/kodak/>, 1999. Accessed: 2025-11-08.

[11] Noam Elata, Tomer Michaeli, and Michael Elad. PSC: Posterior sampling-based compression. In *15th International Conference on Sampling Theory and Applications*, 2025.

[12] Patrick Esser, Robin Rombach, and Bjorn Ommer. Taming transformers for high-resolution image synthesis. In *Proceedings of the IEEE/CVF conference on computer vision and pattern recognition*, pages 12873–12883, 2021.

[13] Marta Gentiloni Silveri, Alain Durmus, and Giovanni Conforti. Theoretical guarantees in kl for diffusion flow matching. *Advances in Neural Information Processing Systems*, 37:138432–138473, 2024.

[14] Ian Goodfellow, Jean Pouget-Abadie, Mehdi Mirza, Bing Xu, David Warde-Farley, Sherjil Ozair, Aaron Courville, and Yoshua Bengio. Generative adversarial networks. *Communications of the ACM*, 63(11):139–144, 2020.

[15] Jinpei Guo, Yifei Ji, Zheng Chen, Kai Liu, Min Liu, Wang Rao, Wenbo Li, Yong Guo, and Yulun Zhang. Oscar: One-step diffusion codec across multiple bit-rates. *arXiv preprint arXiv:2505.16091*, 2025.

[16] Dailan He, Ziming Yang, Weikun Peng, Rui Ma, Hongwei Qin, and Yan Wang. Elic: Efficient learned image compression with unevenly grouped space-channel contextual adaptive coding. In *Proceedings of the IEEE/CVF Conference on Computer Vision and Pattern Recognition*, pages 5718–5727, 2022.

[17] Dailan He, Ziming Yang, Hongjiu Yu, Tongda Xu, Jixiang Luo, Yuan Chen, Chenjian Gao, Xinjie Shi, Hongwei Qin, and Yan Wang. Po-elic: Perception-oriented efficient learned image coding. In *Proceedings of the IEEE/CVF Conference on Computer Vision and Pattern Recognition*, pages 1764–1769, 2022.

[18] Kaiming He, Xiangyu Zhang, Shaoqing Ren, and Jian Sun. Deep residual learning for image recognition. In *Proceedings of the IEEE conference on computer vision and pattern recognition*, pages 770–778, 2016.

[19] Martin Heusel, Hubert Ramsauer, Thomas Unterthiner, Bernhard Nessler, and Sepp Hochreiter. Gans trained by a two time-scale update rule converge to a local nash equilibrium. *Advances in neural information processing systems*, 30, 2017.

[20] Jonathan Ho and Tim Salimans. Classifier-free diffusion guidance. In *NeurIPS 2021 Workshop on Deep Generative Models and Downstream Applications*, 2021.

[21] Jonathan Ho, Ajay Jain, and Pieter Abbeel. Denoising diffusion probabilistic models. *Advances in neural information processing systems*, 33:6840–6851, 2020.

[22] Shoma Iwai, Tomo Miyazaki, Yoshihiro Sugaya, and Shinichiro Omachi. Fidelity-controllable extreme image compression with generative adversarial networks. In *2020 25th International Conference on Pattern Recognition (ICPR)*, pages 8235–8242. IEEE, 2021.

[23] Zhaoyang Jia, Jiahao Li, Bin Li, Houqiang Li, and Yan Lu. Generative latent coding for ultra-low bitrate image compression. In *Proceedings of the IEEE/CVF Conference on Computer Vision and Pattern Recognition*, pages 26088–26098, 2024.

[24] Alexander Kirillov, Eric Mintun, Nikhila Ravi, Hanzi Mao, Chloe Rolland, Laura Gustafson, Tete Xiao, Spencer Whitehead, Alexander C Berg, Wan-Yen Lo, et al. Segment anything. In *Proceedings of the IEEE/CVF international conference on computer vision*, pages 4015–4026, 2023.

[25] Alina Kuznetsova, Hassan Rom, Neil Alldrin, Jasper Uijlings, Ivan Krasin, Jordi Pont-Tuset, Shahab Kamali, Stefan Popov,

Matteo Malloci, Alexander Kolesnikov, et al. The open images dataset v4: Unified image classification, object detection, and visual relationship detection at scale. *International journal of computer vision*, 128(7):1956–1981, 2020.

[26] Nikolai Körber, Eduard Kromer, Andreas Siebert, Sascha Hauke, Daniel Mueller-Gritschneider, and Björn W. Schuller. Perco (sd): Open perceptual compression. *CoRR*, 2024.

[27] Hageyeong Lee, Minkyu Kim, Jun-Hyuk Kim, Seungeon Kim, Dokwan Oh, and Jaeho Lee. Neural image compression with text-guided encoding for both pixel-level and perceptual fidelity. In *International Conference on Machine Learning*, 2024.

[28] Eric Lei, Yigit Berkay Uslu, Hamed Hassani, and Shirin Saeedi Bidokhti. Text + sketch: Image compression at ultra low rates. In *ICML 2023 Workshop Neural Compression: From Information Theory to Applications*, 2023.

[29] Junnan Li, Dongxu Li, Silvio Savarese, and Steven Hoi. Blip-2: Bootstrapping language-image pre-training with frozen image encoders and large language models. In *International conference on machine learning*, pages 19730–19742. PMLR, 2023.

[30] Tianhong Li and Kaiming He. Back to basics: Let denoising generative models denoise. *arXiv preprint arXiv:2511.13720*, 2025.

[31] Zhiyuan Li, Yanhui Zhou, Hao Wei, Chenyang Ge, and Jingwen Jiang. Towards extreme image compression with latent feature guidance and diffusion prior. *IEEE Transactions on Circuits and Systems for Video Technology*, 2024.

[32] Xingchao Liu, Chengyue Gong, and qiang liu. Flow straight and fast: Learning to generate and transfer data with rectified flow. In *The Eleventh International Conference on Learning Representations*, 2023.

[33] Fabian Mentzer, George D Toderici, Michael Tschannen, and Eirikur Agustsson. High-fidelity generative image compression. *Advances in neural information processing systems*, 33: 11913–11924, 2020.

[34] Fabian Mentzer, David Minnen, Eirikur Agustsson, and Michael Tschannen. Finite scalar quantization: VQ-VAE made simple. In *The Twelfth International Conference on Learning Representations*, 2024.

[35] Matthew J Muckley, Alaaeldin El-Nouby, Karen Ullrich, Hervé Jégou, and Jakob Verbeek. Improving statistical fidelity for neural image compression with implicit local likelihood models. In *International Conference on Machine Learning*, pages 25426–25443. PMLR, 2023.

[36] Guy Ohayon, Hila Manor, Tomer Michaeli, and Michael Elad. Compressed image generation with denoising diffusion codebook models. In *Forty-second International Conference on Machine Learning*, 2025.

[37] Maxime Oquab, Timothée Darcet, Théo Moutakanni, Huy Vo, Marc Szafraniec, Vasil Khalidov, Pierre Fernandez, Daniel Haziza, Francisco Massa, Alaaeldin El-Nouby, et al. DINov2: Learning robust visual features without supervision. *Transactions on Machine Learning Research*, 2024.

[38] Robin Rombach, Andreas Blattmann, Dominik Lorenz, Patrick Esser, and Björn Ommer. High-resolution image synthesis with latent diffusion models. In *Proceedings of the IEEE/CVF conference on computer vision and pattern recognition*, pages 10684–10695, 2022.

[39] Olga Russakovsky, Jia Deng, Hao Su, Jonathan Krause, Sanjeev Satheesh, Sean Ma, Zhiheng Huang, Andrej Karpathy, Aditya Khosla, Michael Bernstein, et al. Imagenet large scale visual recognition challenge. *International journal of computer vision*, 115(3):211–252, 2015.

[40] Tim Salimans and Jonathan Ho. Progressive distillation for fast sampling of diffusion models. *arXiv preprint arXiv:2202.00512*, 2022.

[41] Yang Song and Stefano Ermon. Generative modeling by estimating gradients of the data distribution. *Advances in neural information processing systems*, 32, 2019.

[42] Lucas Theis, Tim Salimans, Matthew D Hoffman, and Fabian Mentzer. Lossy compression with gaussian diffusion. *arXiv preprint arXiv:2206.08889*, 2022.

[43] George Toderici, Lucas Theis, Nick Johnston, Eirikur Agustsson, Fabian Mentzer, Johannes Ballé, Wenzhe Shi, and Radu Timofte. Clic 2020: Challenge on learned image compression. *Retrieved March*, 29:2021, 2020.

[44] Ashish Vaswani, Noam Shazeer, Niki Parmar, Jakob Uszkoreit, Llion Jones, Aidan N Gomez, Łukasz Kaiser, and Illia Polosukhin. Attention is all you need. *Advances in neural information processing systems*, 30, 2017.

[45] Jeremy Vonderfecht and Feng Liu. Lossy compression with pretrained diffusion models. In *The Thirteenth International Conference on Learning Representations*, 2025.

[46] VVC-21.2. https://vcgit.hhi.fraunhofer.de/jvet/VVCSoftware_VTM/-/tree/VTM-21.2. Accessed: 10/23/2023, 2023.

[47] Shuai Wang, Ziteng Gao, Chenhui Zhu, Weilin Huang, and Limin Wang. Pixnerd: Pixel neural field diffusion. *arXiv preprint arXiv:2507.23268*, 2025.

[48] Shuai Wang, Zhi Tian, Weilin Huang, and Limin Wang. Ddt: Decoupled diffusion transformer. *arXiv preprint arXiv:2504.05741*, 2025.

[49] Tongda Xu, Ziran Zhu, Dailan He, Yanghao Li, Lina Guo, Yuanyuan Wang, Zhe Wang, Hongwei Qin, Yan Wang, Jingjing Liu, and Ya-Qin Zhang. Idempotence and perceptual image compression. In *The Twelfth International Conference on Learning Representations*, 2024.

[50] Naifu Xue, Zhaoyang Jia, Jiahao Li, Bin Li, Yuan Zhang, and Yan Lu. Dlf: Extreme image compression with dual-generative latent fusion. In *Proceedings of the IEEE/CVF International Conference on Computer Vision (ICCV)*, 2025.

[51] Naifu Xue, Zhaoyang Jia, Jiahao Li, Bin Li, Yuan Zhang, and Yan Lu. One-step diffusion-based image compression with semantic distillation. In *The Thirty-ninth Annual Conference on Neural Information Processing Systems*, 2025.

[52] Ruihan Yang and Stephan Mandt. Lossy image compression with conditional diffusion models. *Advances in Neural Information Processing Systems*, 36:64971–64995, 2023.

[53] Tianwei Yin, Michaël Gharbi, Richard Zhang, Eli Shechtman, Fredo Durand, William T Freeman, and Taesung Park. One-step diffusion with distribution matching distillation. In *Proceedings of the IEEE/CVF conference on computer vision and pattern recognition*, pages 6613–6623, 2024.

- [54] Sihyun Yu, Sangkyung Kwak, Huiwon Jang, Jongheon Jeong, Jonathan Huang, Jinwoo Shin, and Saining Xie. Representation alignment for generation: Training diffusion transformers is easier than you think. In *The Thirteenth International Conference on Learning Representations*, 2025.
- [55] Richard Zhang, Phillip Isola, Alexei A Efros, Eli Shechtman, and Oliver Wang. The unreasonable effectiveness of deep features as a perceptual metric. In *Proceedings of the IEEE conference on computer vision and pattern recognition*, pages 586–595, 2018.
- [56] Tianyu Zhang, Xin Luo, Li Li, and Dong Liu. Stablecodec: Taming one-step diffusion for extreme image compression. In *Proceedings of the IEEE/CVF International Conference on Computer Vision (ICCV)*, pages 17379–17389, 2025.

Appendices

This document provides the supplementary material to Compression-oriented Diffusion foundation model, **CoD**.

A. Towards 64-Bit Image Compression

In this paper, we primarily discuss CoD at 0.0039 bpp, which corresponds to 1024 bits for a 512×512 image. Results demonstrate that the shape, color, and high-level semantic fidelity are well preserved under this bitrate. In this section, we further explore a more extreme compression of 64 bits for a 512×512 image (i.e., 0.00024 bpp) to analyze the boundary of semantic-level compression. To achieve 64 bits, our encoder downsamples the original image to $1/128$ of its original resolution (4×4 patches) and uses a codebook size of $2^4 = 16$. Since latent-space CoD performs better at lower bitrates (Figure 5 in the paper), we train our 64-bit CoD on latent space.



Figure 10. Evaluation of 64-bit CoD on Kodak at 512×512 .

We evaluate our 64-bit CoD on the Kodak dataset in Figure 10. Surprisingly, under such an extremely low bitrate, CoD successfully reconstructs the correct semantics of the original image. By contrast, Stable Diffusion based codecs DDCM [36] and DiffC [45] fail to reconstruct correct semantics even at a fourfold ($4 \times$) higher bit cost. We further leverage DiffC to evaluate the downstream compression performance on Kodak [10] in Figure 11, where CoD-based DiffC significantly outperforms other Stable Diffusion based codecs. Our scheme achieves a FID of 70 with only less than 10% of the bits of prior codecs, highlighting the extreme compression capability of 64-bit CoD.

B. Towards One-Step Diffusion Compression

Preliminary. Recently, one-step diffusion models have demonstrated effectiveness in generative image compression. Unlike multi-step diffusion, which optimizes each diffusion timestep separately, one-step diffusion can be trained end-to-end, enabling better overall performance. OSCAR [15] fine-tuned a multi-step Stable Diffusion to function as a one-step image codec. Subsequently, **one-step diffusion foundation models** have been explored for generative image compression. StableCodec [56] further leverages a one-step SD-Turbo as the foundation model, achieving significantly improved performance. Similarly, OneDC [51] employs a one-step DMD-distilled [53] Stable Diffusion as the foundation model for one-step diffusion compression. The success of these approaches motivates our exploration of CoD in the context of one-step diffusion foundation models.

Since the SD-Turbo distillation process is not fully public, we follow DMD [53] to distill our diffusion model. Given a one-step diffusion network $G_\theta(z)$ that generates x using random noise z , DMD proves that the KL divergence between the real and fake distributions can be expressed as a distribution-matching loss:

$$\nabla_\theta D_{KL} = \mathbb{E}_{\substack{z \sim \mathcal{N}(0; \mathbf{I}) \\ x = G_\theta(z)}} \left[- (s_{\text{real}}(x) - s_{\text{fake}}(x)) \frac{dG}{d\theta} \right], \quad (9)$$

where $s_{\text{real}}(x)$ and $s_{\text{fake}}(x)$ are the score functions [41] of their respective distributions. By adding random noise to x , the score can be predicted by a diffusion model. DMD leverages a pretrained multi-step diffusion model for the real score and dynamically trains a diffusion model to estimate the fake score for one-step samples x .

Distilling a CoD. Following OneDC, we train a one-step CoD using a combination of pixel-space loss and DMD loss:

$$\mathcal{L}_{\text{OS}} = \mathcal{L}_1 + \mathcal{L}_{\text{LPIPS}} + \lambda \cdot \mathcal{L}_{\text{REPA}} + \zeta \cdot \mathcal{L}_{\text{DMD}}, \quad (10)$$

where \mathcal{L}_1 and $\mathcal{L}_{\text{LPIPS}}$ are the pixel-space L1 loss and the VGG [55] LPIPS loss, and $\mathcal{L}_{\text{REPA}}$ is the representation alignment loss. We set $\lambda = 0.5$ and $\zeta = 0.625$. The condition encoder and decoder are kept fixed while tuning the diffusion module, as optimizing the condition during training could introduce discrepancies between the teacher and student models, potentially causing catastrophic training failure.

For simplicity, we optimize only the pixel-space CoD, allowing pixel-space losses to be computed directly. Following the DMD procedure, we update the one-step CoD every 10 steps, while the remaining 9 steps train the fake score diffusion model. The model is trained for 50K steps (i.e., 5K steps for the one-step CoD) with a batch size of 32, which takes approximately 12 hours on 4 A100 GPUs (48 A100 GPU hours in total).

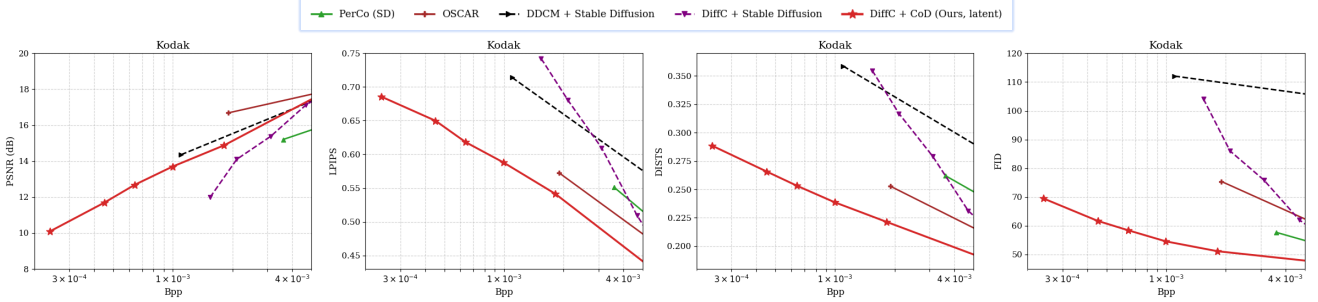


Figure 11. Rate-Distortion comparison for 64-bit CoD and Stable Diffusion based codecs on Kodak at 512×512 .

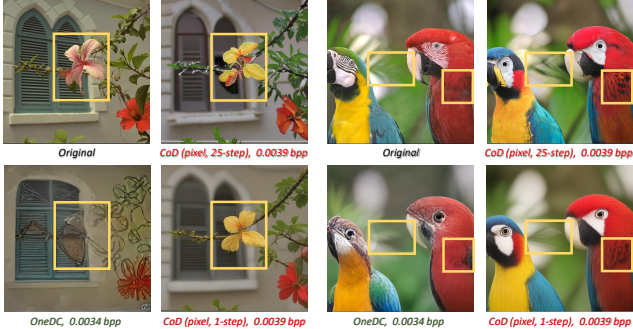


Figure 12. Evaluation of one-step CoD on Kodak at 512×512 .

Evaluation. We evaluate our one-step CoD on Kodak in Figure 12. With very limited training steps, one-step CoD achieves impressive reconstruction quality. Although its detail is not as clear as multi-step CoD, its hue is more similar to the original image, and some structures exhibit higher fidelity. Compared to the DMD-distilled diffusion codec OneDC, one-step CoD has better perceptual quality. The rate-distortion curves tested on Kodak are shown in Figure 14, where one-step CoD showcases better PSNR and LPIPS values than multi-step CoD, while DISTs and FID are slightly worse. Compared to other one-step diffusion codecs, one-step CoD has comparable or better perceptual metrics and a higher PSNR.

Note. In this paper, we train one-step CoD with limited steps (5K generator optimization steps), mainly to explore its properties rather than delivering a fully optimized one-step diffusion codec. Notably, training a one-step Stable Diffusion using DMD costs approximately 1664 A100 GPU hours, whereas we use 48 A100 hours. We believe longer training, a larger batch size, or larger-scale datasets can further boost its performance.

C. Towards Perceptual Supervision via CoD

In the DMD loss in Equation 9, for any input x , we can optimize its KL divergence using CoD to estimate real and fake scores. This indicates that CoD can act as a perceptual supervision mechanism, enhancing the realism of reconstructions for a variety of networks, including other pixel-space codecs, restoration models, or super-resolution models. To

demonstrate this potential, we finetune the pixel-space codec MS-ILLM [35] using the CoD-based DMD loss.

Methods	PSNR	LPIPS*	DISTS	FID
MS-ILLM	21.43 dB	0.403	0.271	92.5
+ CoD-based DMD loss	21.10 dB	0.402	0.255	80.1

* LPIPS is measured with AlexNet. MS-ILLM is trained with LPIPS (Alex), while we follow a more common practice LPIPS (VGG) to avoid train-test overfitting, explaining the minor LPIPS gain.

Table 1. Finetuning the decoder of MS-ILLM using CoD as a perceptual supervision. Evaluated on Kodak at 512×512 . BPP=0.011.

Evaluation. MS-ILLM is typically pretrained using the MSE loss, after which the encoder and entropy model are fixed while the decoder is finetuned with perceptual losses such as LPIPS and GAN [14] loss. Following this paradigm, we finetune only the decoder of MS-ILLM, replacing the GAN loss with the CoD-based DMD loss. Remarkably, after optimizing the decoder for just 2K steps with a batch size of 32 (20K steps total including fake score learning, requiring only about 14 A100 GPU hours), MS-ILLM demonstrates substantially improved realism, as shown in Table 1. The CoD-based DMD loss enhances perceptual metrics, notably reducing FID from 92.5 to 80.1. Several visual examples are presented in Figure 13, where the CoD-based DMD loss markedly reduces artifacts and yields clearer edges and finer details. Since the encoder is fixed, the encoded information remains heavily distorted under MSE-only optimization, resulting in poor overall reconstruction. We expect that jointly tuning the entire network with the CoD-based DMD loss could further improve perceptual quality.

Discussion. Instead of relying on text conditions, CoD learns native image conditions for diffusion. Under DMD supervision, conditions are important since they guide which types of realistic details to generate. Native image conditions provide directions that more closely align with the original image, making CoD theoretically better suited as DMD supervision for reconstruction-related tasks. Moreover, CoD is text-free, eliminating the need for extensive captioning at each optimization step and thereby improving training efficiency. In addition, adopting latent diffusion for DMD loss

is non-trivial for pixel-space codecs, whereas our pixel-space CoD offers a more direct and compatible solution.

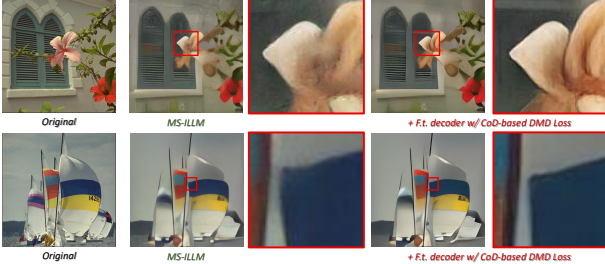


Figure 13. Finetuning MS-ILLM decoder with CoD-based DMD loss.

D. Exploring \mathcal{X} -Prediction Pixel Diffusion

Since \mathcal{V} -prediction (velocity prediction) was proposed [40] and later adopted by Stable Diffusion v2.1, it has become a common practice in latent diffusion models, including the baseline diffusion architectures used in our work [47, 48]. However, recent research by Just Image Diffusion (JiT) [30] shows that pixels lie on a low-dimensional manifold, making \mathcal{X} -prediction a more effective approach for directly modeling pixel distributions. In this paper, we primarily adopt \mathcal{V} -prediction to provide a unified view of latent- and pixel-space compression. Nevertheless, in this section, we conduct experiments to demonstrate that \mathcal{X} -prediction can achieve better reconstruction performance.

Pixel-space CoD with JiT. CoD does not require any specialized network design for the diffusion model, so we can directly replace our pixel-space diffusion model with JiT. We refer to this variant as CoD (pixel- \mathcal{X}) to distinguish it from our velocity-based pixel-space CoD. Following JiT, CoD (pixel- \mathcal{X}) predicts denoised pixels while being trained with a velocity loss, maintaining consistency with our original training objective.

Comparison. We train both CoD (pixel) and CoD (pixel- \mathcal{X}) at 256×256 resolution under identical conditions for 200K steps and evaluate them on Kodak. As shown in Table 2, compared to \mathcal{V} -prediction, we note \mathcal{X} -prediction improves PSNR, LPIPS and DISTS by a large margin, while achieving a comparable FID score. It demonstrates the superiority of \mathcal{X} -prediction in terms of reconstruction fidelity. In future, we will explore \mathcal{X} -prediction for more advanced pixel-space diffusion codecs.

Method @ 0.0156 bpp	PSNR	LPIPS	DISTS	FID
CoD (pixel)	15.00 dB	0.378	0.224	92.7
CoD (pixel- \mathcal{X})	16.99 dB	0.348	0.207	93.4

Table 2. Ablation study for \mathcal{X} -prediction on Kodak at 256×256 . Each model is trained for 200k steps for comparison.

E. Additional Details and Results

This section provides further training details and additional evaluation results, including complexity analysis and visual comparisons.

E.1. Training Details

E.1.1 Datasets

We train the model using three publicly available datasets: **ImageNet-21K** [39] contains 14.2M images across 21K categories. After removing images with a shorter edge below 256 pixels, 9.3M images remain for 256×256 pre-training. **OpenImages** [25] and **SA-1B** [24] provide high-resolution images. We use 1.7M directly downloadable images from OpenImages V4 and all 11.1M images from SA-1B for both 256×256 and 512×512 resolution pre-training. Overall, CoD is trained on 22.1M images. Compared with modern diffusion pipelines, this is a relatively modest data scale, and the only filtering criterion is image resolution rather than extensive data cleaning. We expect that scaling up training with higher-quality data will further improve the performance of CoD.

E.1.2 Unified Training

Section 2.2 (in the paper) emphasizes that unified training is crucial for achieving high reconstruction fidelity. Table 4 reinforces this observation: unified training (ID = C) provides a clear improvement over the baseline (ID = A). Without unified optimization of the condition and diffusion branches, the condition model tends to encode only structural information while neglecting essential color cues. An intuitive workaround is to impose explicit supervision on the condition learning using an auxiliary loss \mathcal{L}_{aux} .

Auxiliary Loss. Given the output of the condition decoder, we attach two lightweight auxiliary prediction heads to (1) reconstruct the input x and (2) predict its DINO v2 [37] representation. The auxiliary objective is

$$\mathcal{L}_{\text{aux}} = \mathcal{L}_{\text{aux}}^{\text{MSE}} + 0.5 \cdot \mathcal{L}_{\text{aux}}^{\text{DINO}} \quad (11)$$

where $\mathcal{L}_{\text{aux}}^{\text{MSE}}$ measures pixel reconstruction accuracy, and $\mathcal{L}_{\text{aux}}^{\text{DINO}}$ promotes feature consistency by maximizing the cosine similarity between predicted and ground-truth DINO representations. Each auxiliary head consists of a lightweight three-layer convolutional module, adding negligible training overhead. All auxiliary heads are removed at inference time. As shown in Table 4, auxiliary supervision alone (ID = B) achieves FID competitive with unified training, but exhibits lower PSNR and LPIPS since the diffusion model does not receive direct distortion supervision.

Unified Post-Training. Motivated by the complementary strengths of unified training and auxiliary supervision, we combine both approaches to further improve performance.

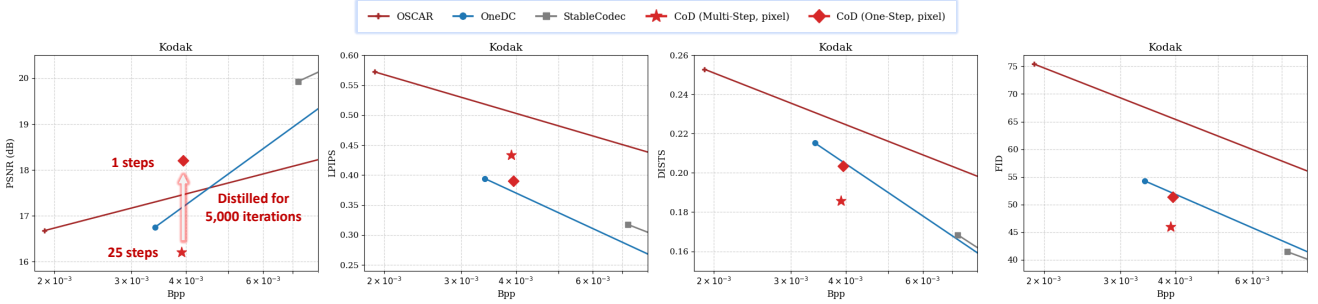


Figure 14. Rate-Distortion comparison for one-step CoD and other one-step diffusion codecs on Kodak at 512×512 .

Method	Stage	Image Resolution	BPP / Total Bits	#Images	Training Steps	Batch Size	Learning Rate	GPU hours (A100)
CoD	Low-Resolution Pre-Training	256×256	0.0156 bpp / 1024 bits	22.1M	400 K	4×32	1×10^{-4}	67
CoD	High-Resolution Pre-Training	512×512	0.0039 bpp / 1024 bits	12.8 M	100 K	4×16	2×10^{-5}	25
CoD	Unified Post-Training	512×512	0.0039 bpp / 1024 bits	12.8 M	50 K	4×16	2×10^{-5}	24

Table 3. Detailed configuration of each CoD training stage. The full training process takes 116 A100 GPU hours (approximately 5 days).

Specifically, we first pre-train CoD with auxiliary loss and then post-train it using unified training. As shown in Table 4, this unified post-training strategy (ID = D) achieves the best overall results among all configurations.

ID	Ablation @ 0.0039 bpp	PSNR	LPIPS	FID
A	Flow matching loss	9.83 dB	0.576	76.8
B	A + Auxiliary Loss	15.20 dB	0.458	48.3
C	A + Unified Training	15.83 dB	0.433	48.4
D	B + Unified Post-Training	16.20 dB	0.433	46.0

Table 4. Ablation study on unified training and auxiliary loss on Kodak at 512×512 .

E.1.3 Multi-Stage Training

In Table 3, we summarize the configuration of all CoD training stages. A key design choice is to keep the total amount of transmitted information fixed across different resolutions. Concretely, we allocate 0.0156 bpp at 0.0156 bpp at 256×256 and 0.0039 bpp at 512×512 , which correspond to the same total bottleneck size of 1024 bits. The codebook size remains unchanged across resolutions. Instead, we change the downsample ratio in the encoder, i.e., $16 \times$ at 256×256 and $32 \times$ at 512×512 .

E.2. Complexity Analysis

Table 5 compares the computational cost of Stable Diffusion v1.5 and CoD. Stable Diffusion requires a large captioning model to generate text conditions, whereas CoD relies on a lightweight 177M image encoder and decoder, taking only 24 ms to process a 512×512 image. The diffusion module in CoD also incurs lower latency and parameter overhead.

Pixel-space CoD is slightly slower than latent-space CoD due to the additional decoupled pixel head, but it avoids the expensive VAE decoding, which makes it faster in the few-step regime.

Despite being faster than Stable Diffusion, the inference speed of CoD remains slow to meet the needs of real-time coding. This limitation can be mitigated by distilling the diffusion process into fewer steps and smaller models. Section B shows the potential of one-step CoD, and Section C demonstrates that CoD can be used as a perceptual supervisory signal. Together, these findings suggest a promising path toward fast inference: **train a lightweight CoD and distill it into a single step using the large CoD as perceptual supervision**. We leave this direction to future work with the goal of real-time diffusion codecs.

Speed (ms) / Params.	Conditioner	Diffusion Module		
		Diffusion	VAE Decoder	Total (25 steps)
Stable Diffusion v1.5	203.0 / 3.7 B*	30.6 / 860 M	43.4 / 49 M	808.4 / 909 M
Latent-space CoD	24.0 / 177 M	21.5 / 676 M	43.4 / 49 M	580.9 / 724 M
Pixel-space CoD	24.0 / 177 M	25.5 / 720 M	0 / 0 M	637.5 / 720 M

* Using BLIP2 captioner with at most 32 tokens, as suggested by PerCo (SD) [26].

Table 5. Complexity comparison with Stable Diffusion. Average speed (ms) is measured for 512×512 on A100.

E.3. Visual Comparison

In Figure 15, we provide more visual comparison examples. Across a wide bitrate range, CoD-based DiffC presents higher perceptual quality than other codecs.

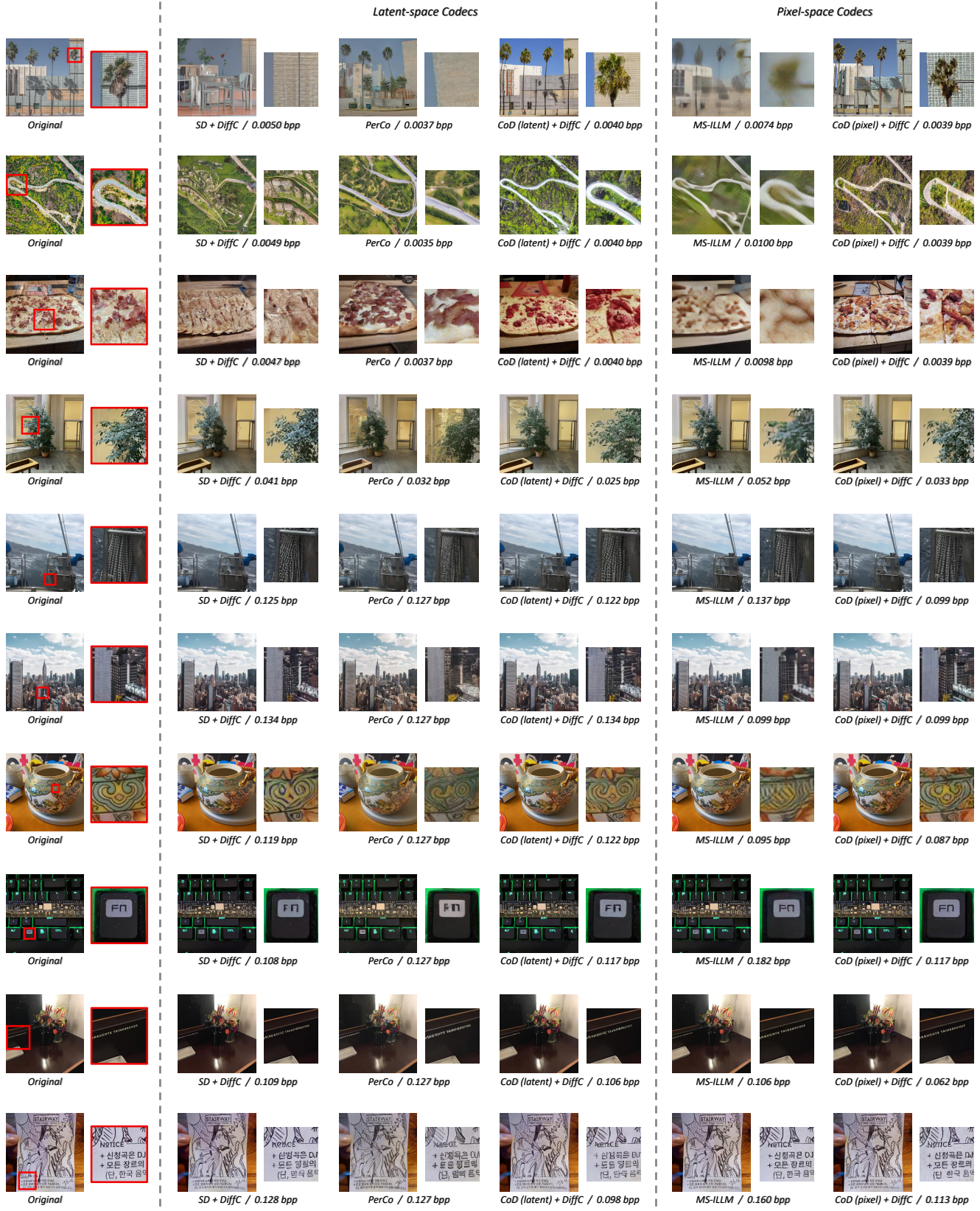


Figure 15. More visualization results on CLIC 2020 test set [43].